



## Sol-gel synthesis and structure of $\text{La}_2\text{O}_3\text{-CoO-SiO}_2$ powders

Lachezar Radev<sup>1</sup>, Liliana Pavlova<sup>1</sup>, Bisserka Samuneva<sup>1\*</sup>, Elena Kashchieva<sup>1</sup>, Irena Mihailova<sup>1</sup>, Maria Zaharescu<sup>2</sup>, Barbara Malic<sup>3</sup>, Luminita Predoana<sup>2</sup>

<sup>1</sup>University of Chemical Technology and Metallurgy, Sofia, Bulgaria

<sup>2</sup>Institute of Physical Chemistry "I.G.Murgulescu", Romania Academy, Bucharest, Romania

<sup>3</sup>Josef Stefan Institute, Ljubljana, Slovenia

Received 15 September 2008; received in revised form 14 November 2008; accepted 29 November 2008

### Abstract

*LaCoO<sub>3</sub> powders are studied because they exhibit interesting electrical, magnetic and catalytic properties. In this paper, new synthesized La<sub>2</sub>O<sub>3</sub>-CoO-SiO<sub>2</sub> powders with different quantity of silica were prepared via sol-gel method in aqua media, starting from metal nitrates with different chelating agents. The relation between the reaction in solution, crystallization pathway and morphology were discussed. In LaCoO<sub>3</sub>-SiO<sub>2</sub> powders, depending on the content of SiO<sub>2</sub> and the treatment temperature (700–1100°C), different crystalline phases (LaCoO<sub>3</sub>, Co<sub>2</sub>SiO<sub>4</sub> and La<sub>9,31</sub>(SiO<sub>4</sub>)<sub>6</sub>O<sub>2</sub>) were observed with the crystallite sizes ranging from 50 to 100 nm. It was proved that chemical composition and nature of used additives has influence on the phase formation and structure of obtained nanomaterials.*

*Keywords: sol-gel synthesis, La<sub>2</sub>O<sub>3</sub>-CoO-SiO<sub>2</sub> powders*

### I. Introduction

Perovskite (LaMeO<sub>3</sub>) type oxide comprising of rare earth ion and *d*-transition metal ions (Me), such as Fe, Mn, Co, Cr, Fe and Ni, has been increasingly applied to devices with improved electric and magnetic properties [1–4]. These compounds have also found application as catalysts for methane combustion reaction and CO oxidation [5]. LaCoO<sub>3</sub>, as one very important member of this group, can be produced by using a lot of methods. Thus, „fused flux” route was used very frequently, but requires high temperatures and long calcination time [6–9]. To dissolve these hard limitations, other techniques were developed. Berger et al. [10] reported that pure and doped LaCoO<sub>3</sub> were obtained by solution combustion method with metal nitrates, and amino acid (alanine) or carbamide as fuel. Taguchi et al. [11,12] synthesized LaCoO<sub>3</sub> using poly(acrylic acid). They noticed that the amount of poly(acrylic acid) had strong influence on the crystal structure of prepared powders [13]. Some authors prepared LaCoO<sub>3</sub> powder with non-alkoxide (nitrate or acetate) metal precursors and citric acid as a chelating agent. They concluded that

the choice of the precursor had strong influence on the morphology of obtained LaCoO<sub>3</sub> powder [14,15]. Citric acid and ethylene glycol have been used as chelating agents for preparing of LaCoO<sub>3</sub> structures, because they formed polymerizable complex, based on the processes of polyesterification [3,5,16,17]. A novel sol-gel method for preparations of LaCoO<sub>3</sub> powders with a Schiff base complex has also been developed by Worayingiong et al. [18].

In addition to the pure LaCoO<sub>3</sub> very interesting system, from the application point of view, is La<sub>2</sub>O<sub>3</sub>-CoO-SiO<sub>2</sub>. In the literature there is not enough information on the sol-gel synthesis, phase formation and structure evolution in this system. Thus, it would be interesting to obtain some new scientific data regarding the sol-gel processing of the La<sub>2</sub>O<sub>3</sub>-CoO-SiO<sub>2</sub>, the formation of different crystalline phases and structure evolution depending on different silica content and calcination temperatures. We suppose that the presence of Si-O-Si network and different crystalline phases from La<sub>2</sub>O<sub>3</sub>-CoO system could provoke the synthesis of new nanocomposites with valuable catalytic, magnetic, electrical and optical properties.

In the present paper the recent results on the sol-gel synthesis and structure of perovskite-type LaCoO<sub>3</sub> and nanocomposites, obtained when different amount of SiO<sub>2</sub>

\* Corresponding author: tel: +35 92 816 3374  
fax: +35 92 868 5488, e-mail: samuneva@uctm.edu

was added to  $\text{La}_2\text{O}_3\text{-CoO}$ , have been reviewed. The main goal is to establish the influence of chemical composition and used additives (chelating agents) on the phase formation and the structure evolution of synthesized materials. The crystallization processes in  $\text{La}_2\text{O}_3\text{-CoO}$  and  $\text{La}_2\text{O}_3\text{-CoO}$  with 10, 20 and 50 wt.%  $\text{SiO}_2$  have been studied in order to obtain more information important for the synthesis of powders with desirable perovskite structure.

## II. Experimental

Different  $\text{LaCoO}_3$  powders were synthesized from  $\text{La}(\text{NO}_3)_3 \cdot 6\text{H}_2\text{O}$  and  $\text{Co}(\text{NO}_3)_2 \cdot 6\text{H}_2\text{O}$  in the presence of chelating agents: i) citric acid, ii) citric acid + polyethylene glycol (PEG), iii) carbamide and iv) glycine. The molar amount of chelating agent was equal to the total molar amount of metal nitrates in solution. The synthesis procedures were as follows: a weighed amount of  $\text{La}(\text{NO}_3)_3 \cdot 6\text{H}_2\text{O}$  and chelating agent was dissolved in distilled water under magnetic stirring for 1h. It was necessary, because chelating agent may form ion associated "inner- and outer-sphere complex" with "clathrate coordination". On one hand, this complex could prevent the aggregation of particles in the obtained mixed sol after adding cobalt salt. On the other hand, the presence of  $\text{NO}_3^-$ , with its preference for bidentate coordination and its hard oxygen donors, has the greatest effect on the conformations of organic molecules used as chelating agent. A stoichiometric amount of  $\text{Co}(\text{NO}_3)_2 \cdot 6\text{H}_2\text{O}$  was added into this inorganic-organic solution. After mixing for 2h, the reactants have formed a complete homogeneous transparent solution sol. Only the samples containing glycine were prepared with slowly addition of  $\text{NH}_4\text{OH}$  in order to adjust the pH value of the solution in the range of  $\sim 7\text{--}8$  and to stabilize the nitrate-chelating agent solution.

$\text{LaCoO}_3$  samples with different  $\text{SiO}_2$  content were synthesized from La- and Co-nitrates (in the presence of carbamide) and tetraethoxysilane (TEOS). In the first step, using the sol-gel synthesis, TEOS was prehydrolysed in the presence of  $\text{CH}_3\text{OH}$  and  $\text{H}_2\text{O}$  using a volume ratio  $\text{TEOS} : \text{CH}_3\text{OH} : \text{H}_2\text{O} = 1 : 1 : 1$ . HCl was used as a catalyst. The hydrolysis reaction of TEOS was carried out under stirring to obtain a transparent silica containing solution. The prehydrolysed TEOS was added "drop to drop" to the  $\text{La}_2\text{O}_3$ -chelating agent-CoO solution. Three  $\text{La}_2\text{O}_3\text{-CoO-SiO}_2$  sols with 10, 20 and 50 wt.%  $\text{SiO}_2$  were prepared using the corresponding quantity of the prehydrolysed TEOS. Without any doubt, the polymerized silica network must rearrange the obtained mixed sol for obtaining good particle size distribution, which can lead to shorter periods of calcinations of the obtained dried gels.

The prepared sols ( $\text{La}_2\text{O}_3\text{-CoO}$  and  $\text{La}_2\text{O}_3\text{-CoO}$  with 10, 20 and 50 wt.%  $\text{SiO}_2$ ) were gelled at  $100^\circ\text{C}/12\text{h}$ , and then heated at  $150\text{--}250^\circ\text{C}$  for another 12h. The obtained black amorphous powders were calcined in tubular furnace under an air flow in the temperature range from  $700^\circ\text{C}$  to  $1100^\circ\text{C}$  for 3h.

The phase formation and structure evolution of the obtained  $\text{LaCoO}_3$  and  $\text{LaCoO}_3\text{-SiO}_2$  powders have been studied by XRD (Bruker D8 Advance, in the  $2\theta$  range of  $10\text{--}80^\circ$ ,  $\text{CuK}\alpha$  - radiation with energy dispersive Sol-X detector), FTIR (IR MATSON 7000-FTIR Spectrometer), TEM (EM-400, Philips) and SEM (JEOL JSM-550, JEOL JFC-1200 fine coater).

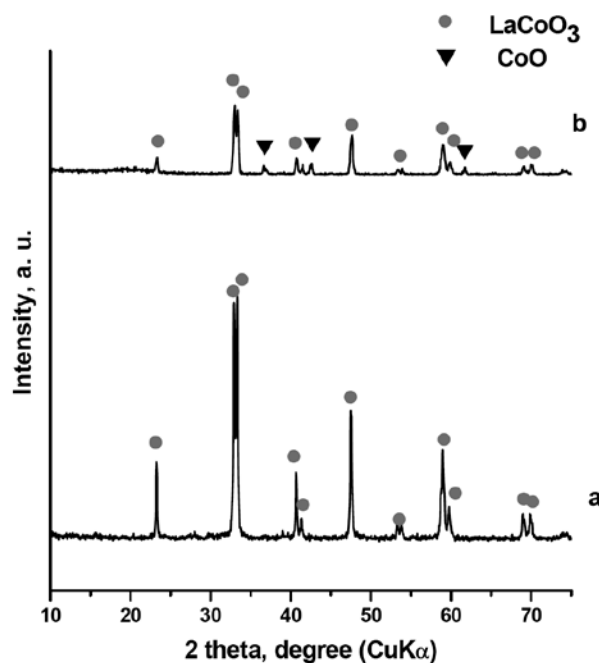


Figure 1. XRD patterns of the  $\text{LaCoO}_3$ , synthesized with carbamide (a) and citric acid + PEG (b), thermal treated at  $700^\circ\text{C}/3\text{h}$

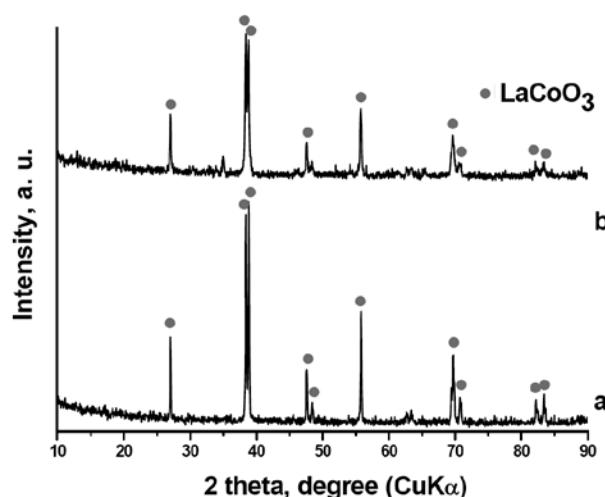


Figure 2. XRD patterns of the  $\text{LaCoO}_3$ , synthesized with citric acid (a) and glycine (b), thermal treated at  $700^\circ\text{C}/3\text{h}$

## III. Results and Discussion

### X-ray diffraction analysis – $\text{La}_2\text{O}_3\text{-CoO}$

The XRD patterns of the synthesized and thermal treated powders are given in Figs. 1–5. The XRD data interpretation was carried out by using JCPDF database.

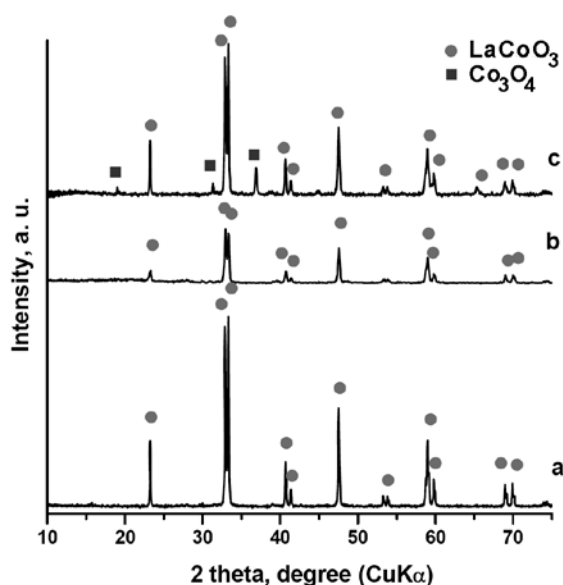


Figure 3. XRD patterns of the  $\text{LaCoO}_3$ , synthesized with carbamide (a), glycine (b), citric acid + PEG, (c), thermal treated at  $900^\circ\text{C}/3\text{h}$

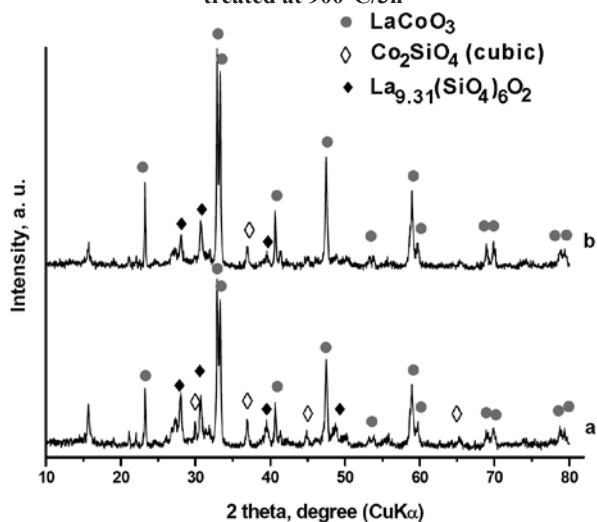


Figure 4. XRD patterns of the  $\text{LaCoO}_3+10\%\text{SiO}_2$ , thermal treated at  $900^\circ\text{C}$  (a) and  $1100^\circ\text{C}$  (b) for 3 h

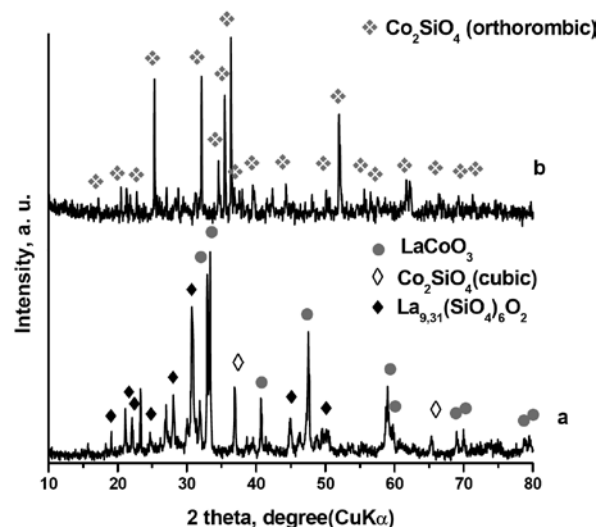


Figure 5. XRD patterns of the  $\text{LaCoO}_3+20\%\text{SiO}_2$ , thermal treated at  $900^\circ\text{C}$  (a) and  $1100^\circ\text{C}$  (b) for 3 h

From the obtained X-ray diffraction data, the crystallinity of samples was estimated by comparing the relative peak intensity of the corresponding crystalline phase.

XRD patterns of the  $\text{La}_2\text{O}_3\text{-CoO}$  samples with different organic additives and thermal treated at  $700^\circ\text{C}/3\text{h}$  are given in Figs. 1 and 2. As can be seen in the presence of carbamide (Fig. 1a), glycine (Fig. 2a) and citric acid (Fig. 2b) the single-phase structure with perovskite  $\text{LaCoO}_3$  phase (PDF 48-0123) was formed. XRD peaks of the samples prepared in presence of carbamide (Fig. 1a) and citric acid (Fig. 2a) have the highest intensity. The synthesized perovskite phase has the rhombohedral symmetry of  $\text{LaCoO}_3$  crystal and nanoscaled size, which was calculated from Scherer's formula and confirmed by TEM and SEM studies. The crystalline sizes obtained by X-ray line bordering were in the range of 50–100 nm depending on the chemical composition and treatment temperature.

Contrary to our results, Popa and Nahikama [17] observed that when  $\text{LaCoO}_3$  was synthesized via amorphous citrate method and thermal treatment at 650 and  $700^\circ\text{C}$ , XRD patterns of the obtained powder consist of some weak unidentified peaks other than  $\text{LaCoO}_3$  phase. Our XRD data are in accordance with the results, presented by Predoana et al. [15], which synthesized  $\text{LaCoO}_3$  powder, without the presence of other phases, using citric acid, metal acetates and nitrates, thermally treated at  $600^\circ\text{C}/6\text{h}$ . Worayingiong et al. [18], reported that the synthesized  $\text{LaCoO}_3$  are characterized by high intensity peaks. The published results, from the same authors, showed no traces of  $\text{La}(\text{OH})_3$  and  $\text{Co}_3\text{O}_4$  in the obtained  $\text{LaCoO}_3$  powders. Bontempi et al. [19] also established, that the increasing in the annealing temperature at  $700^\circ\text{C}$ , resulted in the formation of crystalline pure  $\text{LaCoO}_3$  without the presence of other phases, such as  $\text{La}_2\text{O}_3$ ,  $\text{La}(\text{OH})_3$ ,  $\text{CoO}$  and  $\text{Co}_3\text{O}_4$ . From the published results it can be seen, that the  $\text{La}_2\text{O}_3$  phase would have been observed after annealing the sample at  $1000^\circ\text{C}$  [19]. In the case of citric acid and ethylene glycol, Taguchi et al. [5] reported that the  $\text{LaCoO}_3$  is a main crystalline phase in the synthesized samples.

On the other hand, in the  $\text{La}_2\text{O}_3\text{-CoO}$  powders, synthesized in the presence of citric acid + PEG and heat treated at  $700^\circ\text{C}/3\text{h}$  (Fig. 1b),  $\text{CoO}$  (PDF 48-1719) appears as a secondary phase. The dominant  $\text{LaCoO}_3$  phase has low intensity peaks.

XRD patterns of the  $\text{LaCoO}_3$  synthesized in the presence of carbamide, glycine and citric acid + PEG, thermally treated at  $900^\circ\text{C}/3\text{h}$  are presented in Fig. 3. The pure  $\text{LaCoO}_3$  phase is observed for the samples prepared in the presence of carbamide (Fig 3a) and glycine (Fig. 3b). However,  $\text{Co}_3\text{O}_4$  (PDF 42-1467), can be detected in the  $\text{La}_2\text{O}_3\text{-CoO}$  powder synthesized with citric acid + PEG (Fig. 3c). It can be also seen that the intensity of the  $\text{LaCoO}_3$  peaks depends on the type of the used chelating agents, and decreases as follows: carb-

amide > citric acid + PEG > glycine. The obtained results are in a good agreement with those published by Matei et al. [20], in which  $\text{LaCoO}_3$  was observed as a main phase in the presence of alkali metal chlorides as molten salts thermally treated at  $950^\circ\text{C}$  for 24 h.

#### X-ray diffraction analysis – $\text{La}_2\text{O}_3$ - $\text{CoO}$ - $\text{SiO}_2$

Very interesting new data could be recognised from XRD patterns of the synthesized  $\text{LaCoO}_3$ - $\text{SiO}_2$  powders (in the presence of carbamide) after thermal treatment at  $900^\circ\text{C}$  and  $1100^\circ\text{C}/3\text{h}$  (Figs. 4 and 5). The prepared  $\text{LaCoO}_3$ - $\text{SiO}_2$  powders, depending on the content of  $\text{SiO}_2$  and the treatment temperature ( $700$ – $1100^\circ\text{C}$ ), consist of different crystalline phases:  $\text{LaCoO}_3$ ,  $\text{Co}_2\text{SiO}_4$  (PDF 29-0508) and  $\text{La}_{9,31}(\text{SiO}_4)_6\text{O}_2$  (PDF 76-0340). Thus, in the  $\text{LaCoO}_3$  with 10 wt.%  $\text{SiO}_2$  the dominant perovskite  $\text{LaCoO}_3$  is accompanied with two other phases -  $\text{CoSiO}_4$  and  $\text{La}_{9,31}(\text{SiO}_4)_6\text{O}_2$ . It can be also seen from Fig. 4 that the quantity of secondary silicate phases decreases with increasing temperature from  $900^\circ\text{C}$  to  $1100^\circ\text{C}$ .

In comparison to the  $\text{LaCoO}_3 + 10$  wt.%  $\text{SiO}_2$ , X-ray diffraction patterns of the  $\text{LaCoO}_3 + 20$  wt.%  $\text{SiO}_2$  samples are quite different (Fig. 5). As can be seen, in the  $\text{LaCoO}_3 + 20$  wt.%  $\text{SiO}_2$  powder treated at  $900^\circ\text{C}$  for 3h, perovskite  $\text{LaCoO}_3$  is still the dominant phase (Fig. 5a) and a small portion of  $\text{Co}_2\text{SiO}_4$  and  $\text{La}_{9,31}(\text{SiO}_4)_6\text{O}_2$  can be also observed. However, the  $\text{LaCoO}_3 + 20$  wt.%  $\text{SiO}_2$  powder treated at  $1100^\circ\text{C}/3\text{h}$ , consists of orthorhombic  $\text{Co}_2\text{SiO}_4$  as the major phase, with only a very small portion of other phases, such as:  $\text{LaCoO}_3$  and  $\text{Co}_3\text{O}_4$ .

It is important to mark that the average crystalline size of the  $\text{LaCoO}_3$  phase in the  $\text{LaCoO}_3 + 10$  wt.%  $\text{SiO}_2$  powder is calculated to be about 50 nm and 85 nm at  $900^\circ\text{C}$  and  $1100^\circ\text{C}$ , respectively. However, in the case of the  $\text{LaCoO}_3 + 20$  wt.%  $\text{SiO}_2$  powder, thermally treated at  $900^\circ\text{C}/3\text{h}$ , the size of  $\text{LaCoO}_3$  crystallite increases to 100 nm.

The XRD patterns of the  $\text{LaCoO}_3 + 50$  wt.%  $\text{SiO}_2$  powder (the data are not shown here), thermally treated at  $1100^\circ\text{C}/3\text{h}$ , indicate a very complicated phase composition with the presence of different oxides and silicates of lanthanum and cobalt.

#### Fourier transform infrared spectroscopy (FTIR)

The structure of sol-gel synthesized  $\text{LaCoO}_3$  and  $\text{LaCoO}_3 + 10, 20$  and 50 wt.%  $\text{SiO}_2$  was studied by FTIR (Fig. 6). The FTIR spectrum of the  $\text{LaCoO}_3$  powder, heat treated at  $900^\circ\text{C}/3\text{h}$ , has three characteristic bands at 422, 597 and  $678\text{ cm}^{-1}$ . The two strong absorption bands at about 590 and  $678\text{ cm}^{-1}$  are assigned to Co-O stretching vibration and O-Co-O deformation modes of  $\text{LaCoO}_3$ , respectively [18,21].

La-O bond was assigned to the presence of the absorption band at around  $415$ – $423\text{ cm}^{-1}$  [22]. The FTIR spectra are changed considerably with addition of  $\text{SiO}_2$  (Fig. 6). Thus, in the case of the nanocomposite containing 50 wt.%  $\text{SiO}_2$ , the FTIR spectrum (Fig. 6d) shows the

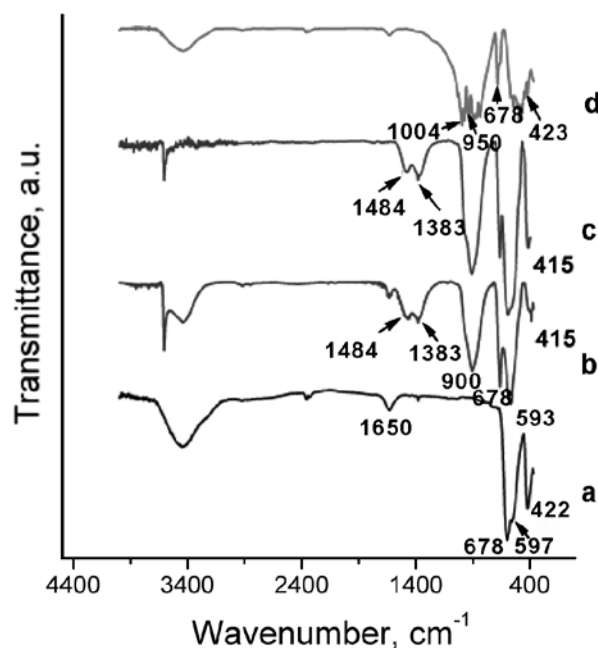
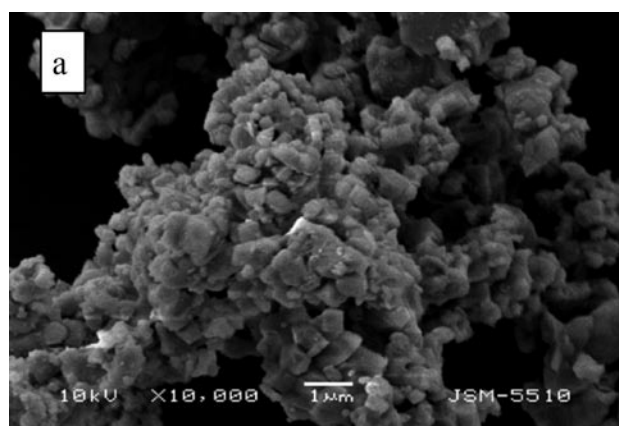
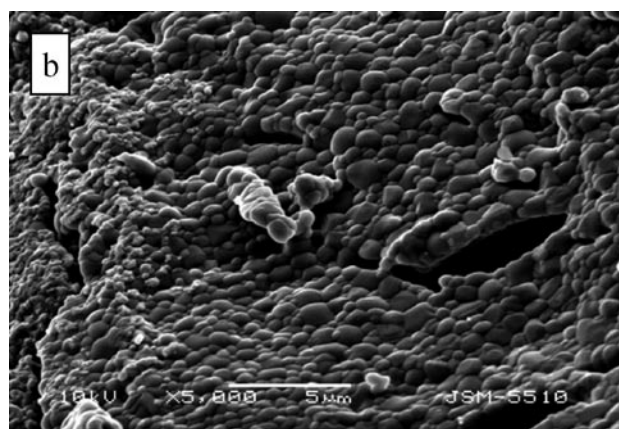


Figure 6. FTIR spectra of  $\text{La}_2\text{O}_3$ . $\text{CoO}$ -glycine at  $900^\circ\text{C}/3\text{h}$  (a),  $\text{La}_2\text{O}_3$ . $\text{CoO}+10\%$  $\text{SiO}_2$  at  $900^\circ\text{C}/3\text{h}$  (b),  $\text{La}_2\text{O}_3$ . $\text{CoO}+10\%$  $\text{SiO}_2$  at  $1100^\circ\text{C}/3\text{h}$  (c) and  $\text{La}_2\text{O}_3$ . $\text{CoO}+50\%$  $\text{SiO}_2$  at  $800^\circ\text{C}/3\text{h}$  (d)



a)



b)

Figure 7. Microstructure of the samples: SEM image of  $\text{LaCoO}_3$  (glycine) at  $900^\circ\text{C}/3\text{h}$  (a); SEM image of  $\text{LaCoO}_3$ -20% $\text{SiO}_2$  (carbamide) heat treated at  $1100^\circ\text{C}/3\text{h}$  (b)

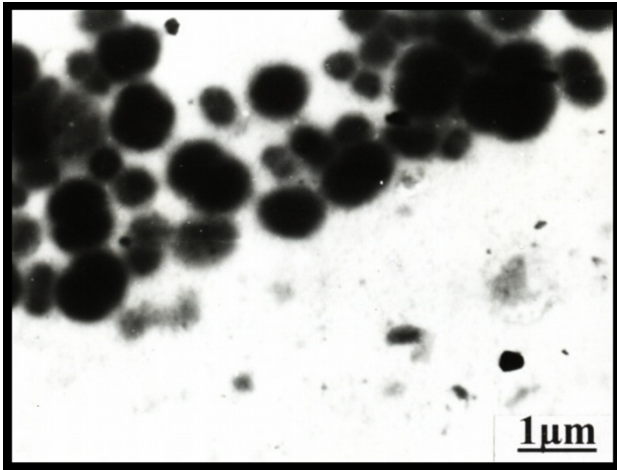


Figure 8. TEM image of  $\text{LaCoO}_3$  (citric acid + PEG) at  $900^\circ\text{C}/3\text{h}$  (c)

bands at  $950\text{ cm}^{-1}$ , attributed to Si-OH groups and  $1004\text{ cm}^{-1}$  assigned to  $\nu_{\text{as}}$  Si-O-Si stretching vibration. This bond shifts to lower wave number in the nanocomposite with 10 wt.%  $\text{SiO}_2$ . The FTIR spectrum of the  $\text{La}_2\text{O}_3$ -CoO powder with 10 wt.%  $\text{SiO}_2$ , treated at  $900^\circ\text{C}$  and  $1100^\circ\text{C}$  for 3h (Fig. 6b,c) the strong chemical bond at  $1484\text{ cm}^{-1}$  can also be observed. This bond could be assigned to Co-O stretching vibrations [23].

#### Scanning Electron Microscopy (SEM)

The morphology of the particles in the obtained  $\text{La}_2\text{O}_3$ -CoO- $\text{SiO}_2$  powders after calcination at different temperatures is determined by SEM (Fig. 7) and TEM (Fig. 8) observations. It is established that the particle size varies from 70–100 nm (for crystallites) to  $1\text{ }\mu\text{m}$  (for aggregates) and their shape depends on the sample composition and heat treatment temperature. Only in the sample  $\text{LaCoO}_3 + 20\text{ wt.}\% \text{SiO}_2$  the particles are with nanoscale sizes, without aggregation trend and with a lower contrast image.

#### IV. Conclusions

Different  $\text{LaCoO}_3$  powders were prepared by the sol-gel technique from lanthanum and cobalt nitrates and in the presence of chelating agents: i) citric acid, ii) citric acid + polyethylene glycol (PEG), iii) carbamide and iv) glycine.  $\text{LaCoO}_3$  single phase composition with rhombohedral distorted perovskite structure is observed in the sol-gel samples prepared in the presence of carbamide, citric acid and glycine, and thermal treated at  $700^\circ\text{C}$  and  $900^\circ\text{C}$ . From the depicted XRD data the high intensity peaks of the obtained  $\text{LaCoO}_3$ , after thermal treatment at  $900^\circ\text{C}$ , are decreased as follows: carbamide > citric acid + PEG > glycine.

New nanocomposites in the  $\text{La}_2\text{O}_3$ -CoO- $\text{SiO}_2$  system with 10, 20 and 50 wt.%  $\text{SiO}_2$  were synthesized via modified sol-gel method. The obtained powders were prepared from lanthanum and cobalt nitrates, carbamide, TEOS,  $\text{CH}_3\text{OH}$ ,  $\text{H}_2\text{O}$  and HCl. In the synthesized  $\text{LaCoO}_3$ - $\text{SiO}_2$  powders, depending on the content

of  $\text{SiO}_2$  and treatment temperature ( $700$ – $1100^\circ\text{C}$ ) different crystalline phases, such as  $\text{LaCoO}_3$ ,  $\text{Co}_2\text{SiO}_4$  and  $\text{La}_{9,31}(\text{SiO}_4)_6\text{O}_2$ , are observed.  $\text{LaCoO}_3$  is indicated as a main crystalline phase, which is accompanied with two other phases -  $\text{CoSiO}_4$  and  $\text{La}_{9,31}(\text{SiO}_4)_6\text{O}_2$  for the samples:  $\text{LaCoO}_3 + 10\text{ wt.}\% \text{SiO}_2$  thermally treated at  $900^\circ\text{C}$  and  $1100^\circ\text{C}$ , and  $\text{LaCoO}_3 + 20\text{ wt.}\% \text{SiO}_2$  at  $900^\circ\text{C}$ . On the other side, the sample  $\text{LaCoO}_3 + 20\text{ wt.}\% \text{SiO}_2$  treated at  $1100^\circ\text{C}$  has the orthorhombic  $\text{Co}_2\text{SiO}_4$  as a dominant phase. The crystallite sizes of the obtained phases are from 50 to 100 nm. Taking into consideration the chemical and phase compositions, as well as their structure, it is supposed that new sol-gel nanocomposites possess valuable catalytic, magnetic, electrical and optical properties.

It has been proved the influence of chemical composition and nature of used additives on the phase formation and structure of obtained  $\text{La}_2\text{O}_3$ -CoO and  $\text{La}_2\text{O}_3$ -CoO- $\text{SiO}_2$  nanomaterials.

**Acknowledgements:** The support from the Bulgarian National Science Fund, Contract VU-TN-102/2005 is greatly acknowledged.

#### References

1. U. Russo, L. Nodari, V. Kuneser, G. Filoti, "Local interactions and electronic phenomena in substituted  $\text{LaFeO}_3$  perovskites", *Solid State Ionics*, **176**, (2005) 97.
2. A.E. Giannakas, A.C. Ladavos, P.J. Pomonis, "Preparation, characterization and investigation of catalytic activity for NO+CO reaction of  $\text{LaMnO}_3$  and  $\text{LaFeO}_3$  perovskites prepared via microemulsion method", *Appl. Catal.:B Environ.*, **49** [3] (2004) 144.
3. M. Popa, J. Frantii, M. Nakihana, "Characterization of  $\text{LaMeO}_3$  (Me: Mn, Co, Fe) perovskite powders obtained by polymerizable complex method", *Solid State Ionics*, **154-155** (2002) 135.
4. X. Qui, J. Zhou, Z. Yue, L. Gui, L. Li, "Auto-combustion synthesis of nanocrystalline  $\text{LaFeO}_3$ ", *Mater. Chem. Phys.*, **78** (2003) 25.
5. H. Taguchi, S. Yamasaki, A. Itadani, M. Yoshinaga, K. Hitora, "CO oxidation on perovskite type  $\text{LaCoO}_3$  synthesized using EG and CA", *Catal. Commun.*, **9** (2008) 1913.
6. C. Chen, F. Wondre, J. Ryan, A. Samanta, "Growth mechanism and additive effect of high- $T_c$  superconducting crystals", *J. Cryst. Growth*, **237-239** (2002) 772.
7. W. Gunter, W. Paulus, R. Schollhorn, "Correlation between synthesis, stoichiometry, structure and superconductivity of  $\text{La}_{2-x}\text{K}_x\text{CuO}_{4-\delta}$ ", *Physica C*, **312** (1999) 61.
8. Md. M. Seikh, L. Sudheendra, Ch. Narayana, C.N.R. Rao, "A raman study of temperature induced low to intermediate spin state transition in  $\text{LaCoO}_3$ ", *J. Mol. Struct.*, **706** (2004) 121.
9. M. Radovich, S.A. Speakman, L. Allard, E. Paysant, E. Lasa-Curzio, M. Kriven, J. Lloyd, L. Fegely, N. Orlovskaya, "Thermal, mechanical and phase stability of  $\text{LaCoO}_3$ ", *J. Powder Sources*, **184** [1] (2008) 77.

10. D. Berger, C. Matei, F. Papa, G. Voicu, V. Fruth, "Pure and doped LaCoO<sub>3</sub> obtained by combustion method", *Prog. Solid State Chem.*, **35** (2007) 183.
11. H. Taguchi, D. Matsuda, M. Nagao, K. Tanihata, Y. Miyamoto, "Synthesis of perovskite-type (La<sub>1-x</sub>Sr<sub>x</sub>)MnO<sub>3</sub> (0 < x < 0.3) at low temperature", *J. Am. Ceram. Soc.*, **75** (1992) 201.
12. H. Taguchi, H. Yoshioka, M. Nagao, "Synthesis of perovskite-type LaCoO<sub>3</sub> using poly(acrylic acid)", *J. Mater. Sci. Lett.*, **13** [12] (1994) 891.
13. H. Taguchi, H. Yoshioka, D. Matsuda, M. Nagao, "Crystal structure of LaMnO<sub>3</sub> synthesized using poly(acrylic acid)", *J. Solid State Chem.*, **104** [2] (1995) 460.
14. H. Taguchi, S. Yamada, M. Nagao, Y. Ichikawa, K. Tabata, "Surface characterization of LaCoO<sub>3</sub> synthesized using citric acid", *Mater. Res. Bull.*, **37** (2002) 69.
15. L. Predoana, B. Malic, M. Kosec, M. Carata, M. Caldararu, M. Zaharescu, "Characterization of LaCoO<sub>3</sub> powders obtained by water based sol-gel method with citric acid", *J. Eur. Ceram. Soc.*, **27** (2007) 4407.
16. M. Popa, Le Van Hong, M. Kakihana, "Nanopowders of LaMeO<sub>3</sub> perovskites", *Physica B*, **327** (2003) 233.
17. M. Popa, M. Kakihana, "Synthesis of LaCoO<sub>3</sub> by the polymerizable complex route", *Solid State Ionics*, **151** (2002) 251.
18. A. Worayingyong, P. Kangvansura, S. Kityakarn, "Schiff base complex sol-gel method for LaCoO<sub>3</sub> perovskite preparation", *Colloid Surface A: Physicochem. Eng. Aspects*, **320** (2008) 123.
19. E. Bontempi, L. Armelao, D. Barreca, L. Bertolo, G. Bottaro, E. Pierangelo, L.E. Depero, "Structural characterization of sol-gel lanthanum cobaltite thin films", *Crystal Eng.*, **5** (2002) 291.
20. C. Matei, D. Berger, P. Marote, S. Stoleriu, J. Deloume, "Lanthanum based perovskites obtained in molten nitrates of nitrites", *Prog. Solid State Chem.*, **35** (2007) 203.
21. M. Khalil, "Synthesis, X-ray, infrared spectra and electrical conductivity of La/Ba-CoO<sub>3</sub> systems", *Mater. Sci. Eng. A*, **352** (2003) 64.
22. D. Berger, N. van Landschoot, C. Ionica, F. Papa, V. Fruth, "Synthesis of pure and doped lanthanum cobaltite by the combustion method", *J. Optoelectron. Adv. Mater.*, **5** [3] (2003) 719.
23. R. Diaz, M.D. Lazo, "Spectroscopic study of CuO/CoO catalysts supported by Si-Al-Y zeolite matrices prepared two sol-gel methods", *J. Sol-Gel Sci. Techn.*, **17** (2000) 137.